

A kinetic and mechanistic study of thermal decomposition of strontium titanate oxalate

B. Sairam Patra, S. Otta, S.D. Bhattamisra*

Department of Chemistry, Berhampur University, Berhampur 760007, Orissa, India

Received 8 September 2005; received in revised form 21 September 2005; accepted 15 November 2005

Available online 6 January 2006

Abstract

Thermal decomposition of anhydrous strontium titanate oxalate proceeds through a series of complex reactions to form strontium metatitanate at high temperature. Among them the decomposition of oxalate is the first major thermal event. A kinetic study of oxalate decomposition in the temperature range 553–593 K has been carried out by cooled gas pressure measurement in vacuum. Results fitted the Zhuravlev equation for almost the entire α -range (0.05–0.92) indicating the occurrence of a diffusion-controlled, three-dimensional rate process. The activation energy has been calculated to be $164 \pm 10 \text{ kJ mol}^{-1}$. Results from elemental analysis, TGA, IR and SEM studies of undecomposed and partially decomposed samples have been used to supplement kinetic observations in formulating the mechanism for oxalate decomposition.

© 2005 Elsevier B.V. All rights reserved.

Keywords: Strontium titanate oxalate; Kinetic studies; Electron microscopy; Mechanism of decomposition; Zhuravlev equation

1. Introduction

Thermal decomposition of strontium titanate oxalate tetrahydrate to strontium titanate is known to involve multi-step complex reactions [1–3]. Different schemes for the decomposition have been proposed. However, in spite of many investigations, little information is available on the kinetics of the decomposition process. The various schemes proposed for the decomposition of strontium titanate oxalate broadly classify the thermal process to proceed through three stages. These include dehydration, followed by decomposition of the oxalate to form a mixed oxide-carbonate, which decomposes at high temperatures to form the metal titanate. Strontium titanate has a perfect perovskite structure with a tolerance factor $t = 1.02$ [4,5]. This factor contributes to the interesting electrical properties of metal titanates and those with $t > 1.0$ tend to be ferroelectric. Because the temperature of calcination of the precursor is known to influence the electrical properties of metal titanates [6,7], a systematic kinetic study of the thermal process is of value.

2. Experimental

Strontium titanate oxalate tetrahydrate (STOT) was prepared by the modified method [8,9] of Claubaugh et al. [10]. The sample was analysed for C (12.03%) and H (2.19%) as against the theoretical values C: 12.01% and H: 2.02% for the molecular formula $\text{SrTiO}(\text{C}_2\text{O}_4)_2 \cdot 4\text{H}_2\text{O}$. The oxalate content was determined by dissolving known amount of the sample in dilute perchloric acid and titrating the hot solution against 0.01N potassium permanganate. It was found to be 2.04 mol/mol of the sample. The same procedure was also adopted for determining oxalate content in partially decomposed samples. Atomic absorption studies indicated strontium and titanium contents as 460 ± 9.0 and $275 \pm 21 \text{ ppm}$ in a $5.25 \times 10^{-3} \text{ mol dm}^{-3}$ acidified solution of STOT as against the corresponding theoretical values of Sr: 460 ppm and Ti: 251 ppm. The high titanium content may be due to its lack of sensitivity towards the technique, although presence of very small amounts of titanium dioxide cannot be ruled out.

Dehydration of the prepared sample was carried out at 473 K in an air oven till constant mass was attained. The final product was 99% dehydrated as determined by C, H analysis and oxalate determination. The IR spectrum of the dehydrated STO had a prominent peak at 1675 cm^{-1} ($\nu_{\text{as}} > \text{C}=\text{O}$), a small peak at 904 cm^{-1} ($\nu_{\text{as}} \text{ C}-\text{C}$) and multiple peaks in the

* Corresponding author. Tel.: +91 680 2242201.

E-mail address: sreelekha_bu@yahoo.com (S.D. Bhattamisra).

zone 1000–1500 cm^{-1} . Partly decomposed samples contained an additional peak at 2334 cm^{-1} ($\nu_{\text{as}} \text{CO}_2$). Here the small peak at 904 cm^{-1} was missing and the $\nu_{\text{as}} > \text{C}=\text{O}$ band was shifted to 1668 cm^{-1} indicative of C–C bond rupture and oxalate breakdown.

The detailed experimental technique used to measure the evolved-gas pressure as a function of time has been described previously [9–11]. Liquid nitrogen and acetone slurry traps were used to measure the pressure values, respectively, of CO and that of CO + CO₂ together. Undecomposed STO and partially decomposed samples were examined in a JEOL35 CF scanning electron microscope for surface features. Oxalate contents, in samples decomposed to different extents, were determined by titration with standard potassium permanganate solution.

3. Results and discussion

3.1. Electron microscopic studies

Representative photographs from microscopic studies of the surfaces of both undecomposed and thermally decomposed (at 584 K) samples of STO reveal that the dehydrated sample consists of aggregates of small crystals (5–10 μm) having rectangu-

lar features with planar surfaces as shown in Fig. 1a. Occasional line cracks might have originated as routes of escape for the water vapour. At 10% decomposition (Fig. 1b) the planar surface features of the crystallites are still retained, but the line cracks become more prominent and the surface is covered with minute spherical eruptions. At 40% decomposition (Fig. 1c), the spherical eruptions are seen to have grown into mushroom-like growths with rounded outlines. At the completion of oxalate decomposition (Fig. 1d) these growths cover the entire surface area and overlap one another. The bulk of the sample apparently has a high degree of porosity and emptiness within. The most obvious explanation to the above findings is instantaneous nucleus formation all over the surface. The nuclei are soon converted into fluid matrices from which the volatile compounds viz. CO and CO₂ escape. The matrix thereafter hardens leaving globular growths on the surface.

3.2. Reaction stoichiometry

On heating in air at 610 K to constant mass the reactant mass-loss for STO is found to correspond to Eq. (1):

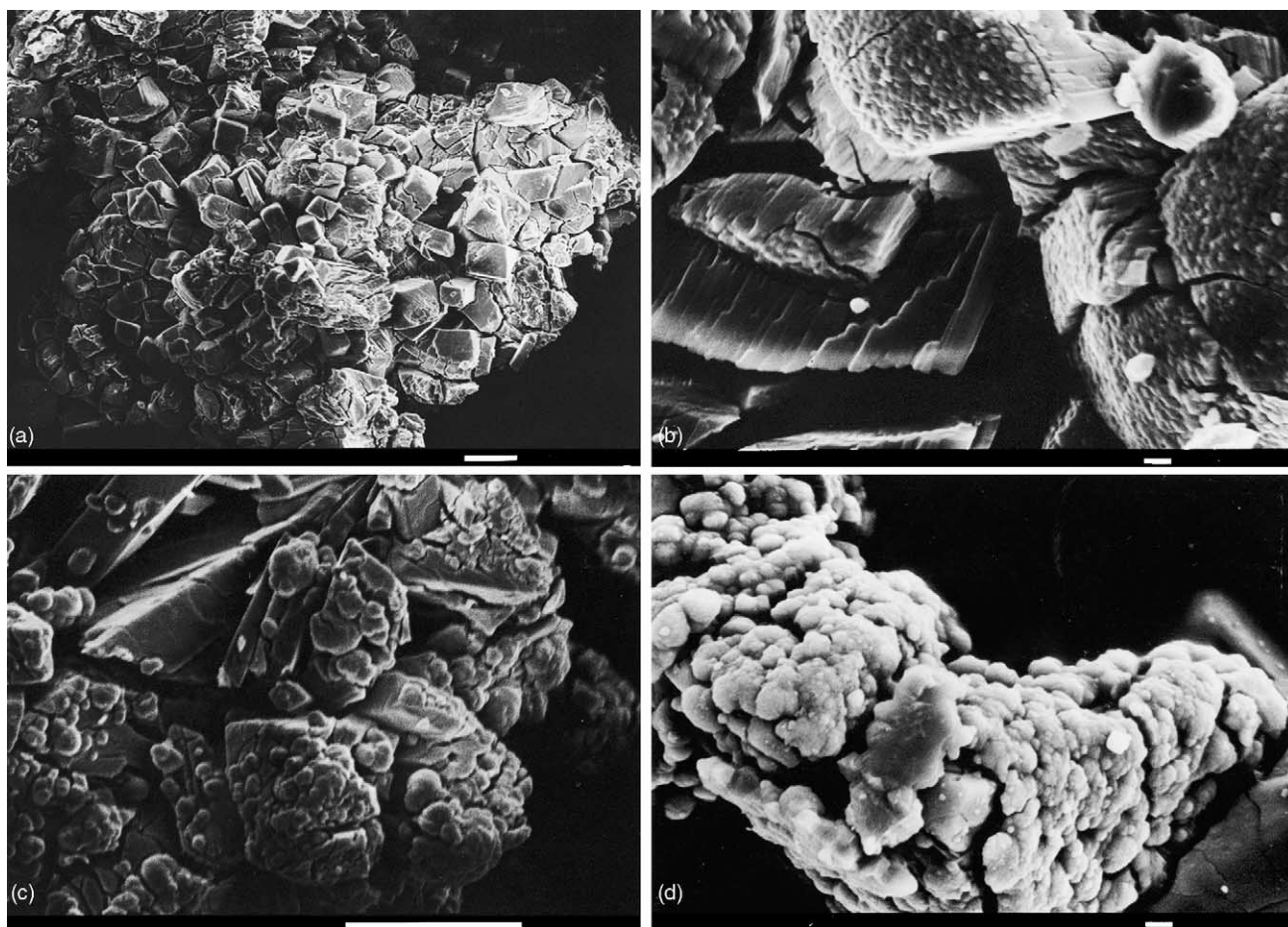
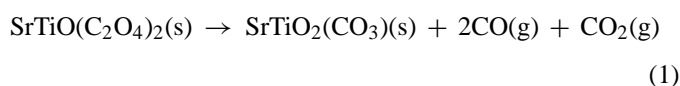


Fig. 1. (a) SEM studies of the surface of dehydrated and undecomposed STO sample; scale bar = 10.0 μm . (b) Partially decomposed STO ($\alpha = 0.10$) at 584 K; scale bar = 1.0 μm . (c) Partially decomposed STO ($\alpha = 0.4$) at 584 K; scale bar = 10.0 μm . (d) SEM studies of the surface of almost completely decomposed STO ($\alpha \approx 1.0$) at 584 K; scale bar = 1.0 μm .

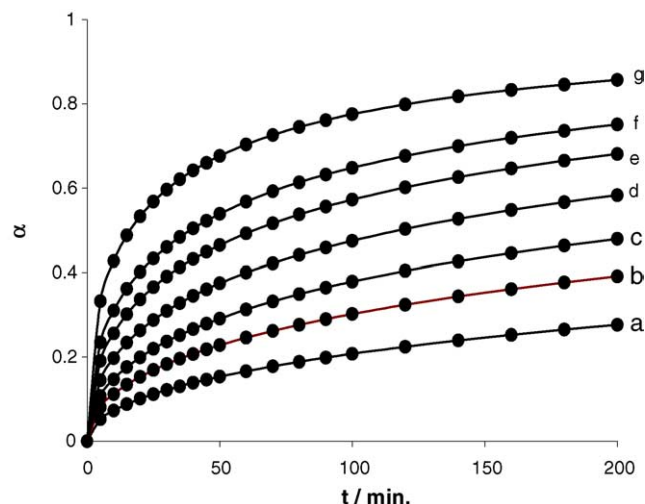
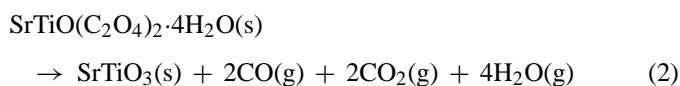


Fig. 2. The α against time plots from CO pressure measurements in vacuum for the thermal decomposition of STO at different temperatures: (a) 533 K, (b) 553 K, (c) 564.5 K, (d) 574.3 K, (e) 584 K, (f) 593 K, and (g) 610 K.

Pressure measurements in vacuum at 610 K confirm that about 97% decomposition with formation of both CO and CO₂ as the volatile products has occurred. Thermogravimetric analysis in air of hydrated strontium titanyl oxalate SrTiO(C₂O₄)₂·4H₂O, in air shows four major mass-loss events. Below 473 K, there is an 18.80(±0.15)% mass-loss presumably due to dehydration (theoretical mass-loss 18.02%). This is followed by two overlapping steps with 7.10 and 17.82% mass-losses, respectively, in temperature range of 473–673 K. Close to 973 K there is a sharp mass-loss event of 11.03%. The total mass-loss is 54.75%, which is in good agreement with the calculated value of 54.05% loss corresponding to escape of volatile products in an overall reaction presented in Eq. (2):



3.3. Evolved-gas pressure measurement

Representative α -time graphs (Fig. 2) for the isothermal decomposition of STO, using a liquid nitrogen trap, are predominantly deceleratory ($\alpha = P/P_f$, where P and P_f refer, respectively, to the pressure value at anytime t and at the end of the reaction). Two distinct processes are evident and these include a rapid initial gas evolution followed by a long deceleratory process. The corresponding $d\alpha/dt$ values reach a maximum within the first few minutes of heating. This time to the maximum decreases with increase in temperature (29 min at 553 K to 5 min at 610 K). However, the maximum value of $d\alpha/dt$ is obtained at a constant α value of 0.15 ± 0.01 , irrespective of the temperature. Representative α - t graphs for CO₂ evolution have the same characteristic features as those for CO evolution. However, CO₂ evolution decreases at longer times, i.e. in the deceleratory stages. Pre-treatment, like crushing and pre-irradiation, hardly change the deceleratory character of the α - t graphs.

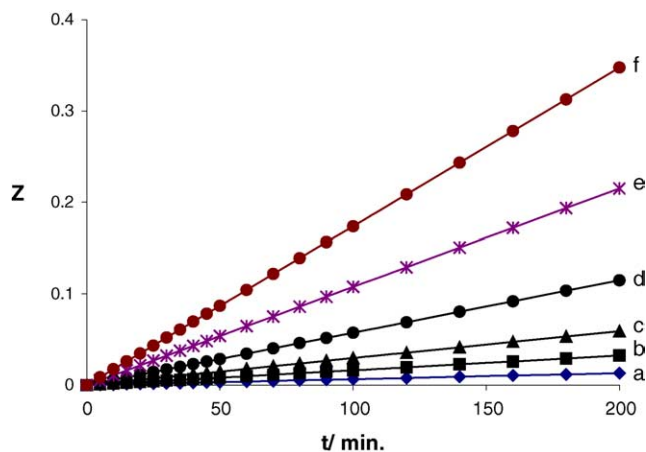


Fig. 3. Plots of $Z = [(1 - \alpha)^{-1/3} - 1]^2$ against time at different temperatures: (a) 533 K, (b) 553 K, (c) 564.5 K, (d) 574.3 K, (e) 584 K, and (f) 593 K.

The α - t graphs are best described by the Zhuravlev equation [12] (Eq. (3)):

$$[(1 - \alpha)^{-1/3} - 1]^2 = kt \quad (3)$$

with a single value for the rate constant for the entire course of decomposition (Fig. 3). The values of the rate constant at different temperatures and the energy of activation for oxalate decomposition are listed in Table 1.

3.4. Reaction mechanism

Titanyl oxalate decomposes to titanium dioxide and carbon monoxide in the temperature range 523–573 K [13,14], while the decomposition of strontium oxalate to carbonate and carbon monoxide occurs [15] at 676 K with an activation energy of 250 kJ mol⁻¹ [16]. Strontium titanyl oxalate, on the other hand, undergoes almost 100% decomposition (Table 1) at 610 K with an activation energy of 164.2 ± 10 kJ mol⁻¹.

In order to propose a mechanism for the oxalate decomposition stage of STO, it may be noted that the decomposition proceeds differently in air and in vacuum. The following points are noteworthy:

1. In vacuum, the pressure values of CO and CO₂ at $(d\alpha/dt)_{\text{max}}$ show that the ratio is almost 1:1 over the entire temperature range of study; however, the ratio falls to 1:0.83 in the deceleratory stage.

Table 1
Rate constants and Arrhenius activation energy for oxalate decomposition using Zhuravlev equation

T (K)	α -range	$k \times 10^4$ (min ⁻¹)	E (kJ mol ⁻¹)
533.0	0.05–0.36	0.650	
553.0	0.08–0.49	1.621	
564.5	0.11–0.59	2.958	164.2 ± 10
574.3	0.15–0.69	5.737	
584.0	0.19–0.78	10.756	
593.0	0.23–0.84	17.378	

Table 2
Calculated and observed pressure values for CO and CO + CO₂ together at different temperatures

T (K)	Decomposition (%)	Pressure (Torr)				$R = p/P$	q	P_c^b (Torr)
		Observed		Calculated ^a				
		CO (p)	CO + CO ₂ (P)	CO (p')	CO + CO ₂ (P')			
553.0	51	1.36	2.43	1.76	2.65	0.56	0.45	2.44
563.5	65	1.61	2.93	2.16	3.23	0.55	0.51	2.97
574.3	73	1.90	3.50	2.54	3.81	0.54	0.50	3.51
584.0	82	2.12	3.92	2.85	4.28	0.54	0.51	3.94
593.3	92	2.38	4.36	3.16	4.74	0.55	0.49	4.36
610.0	97	2.50	4.60	3.35	5.03	0.54	0.51	4.63

^a Calculated using Eq. (9).

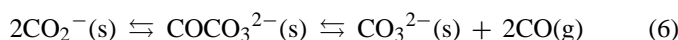
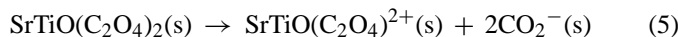
^b Calculated using Eq. (10).

- TG studies in air yield positive information of evolution of only CO in the initial stage, followed by evolution of both CO and CO₂.
- The residue of decomposition in vacuum has a brownish-black colour and the presence of elemental carbon is detected. However, decomposition in air leaves a white residue with no trace of carbon in it.

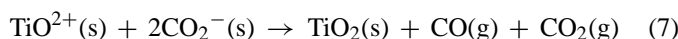
If it is assumed that CO and CO₂ are evolved in equimolar quantities during the initial fast reaction followed by evolution of one more mole of CO in the subsequent slow step, the ratio of CO:CO₂ pressure would be 2:1 instead of 1.205:1 as in the present study. The presence of elemental carbon in the residue of decomposition in vacuum may suggest the occurrence of disproportionation as per Eq. (4):



It has been shown [13,17,18] that the first process in the decomposition of most oxalates is the rupture of the C–C bond. Rotation of the carboxyl group around the axis of symmetry results in the change of group from planar C_{2h} to non-planar C_s with strain sufficient to break the C–C bond. Evidence for the rupture of C–C bond has also been reported in the present study from the IR spectrum of a partially decomposed sample. Accordingly, the scheme of reaction can be presented as



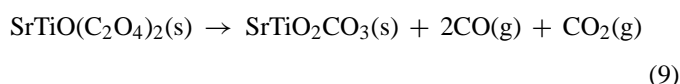
One of the oxalate ions breaks to form CO₂ radicals which isomerise and generate CO in equilibrium steps [13]. In vacuum, once equilibrium is attained, further formation of CO through Eq. (6) is hindered, whereas the reaction proceeds unabated in a flowing atmosphere of air. Thus, for decomposition in vacuum, the reaction in Eq. (6) soon stops; the unstable CO₂ radicals rather combine with TiO²⁺ to form stable gaseous products through electron transfer:



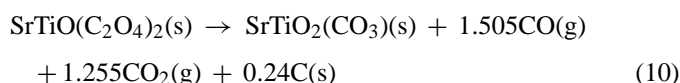
Simultaneous decomposition of the second oxalate ion results in the formation of a mixed oxide carbonate and CO:



The overall decomposition reaction in vacuum can thus be represented by the following equation:



The extent of disproportionation ‘ q ’ in mol/mol (Eq. (4)) is calculated using: $q = 2 [(p' - p)/p']$ where p' is the expected CO pressure as per Eq. (9) and p is the observed CO pressure (using a liquid N₂ trap) at that temperature. At each temperature, the expected CO pressure is determined from the percentage of oxalate decomposition, the latter being estimated by titrating the residual oxalate with standard KMnO₄. These values are presented in (Table 2) from which the value of ‘ q ’ is calculated to be 0.48 ± 0.03 . Thus, about 0.5 mol of CO is converted into CO₂ and elemental carbon by disproportionation. Including the value of ‘ q ’ in Eq. (9), the stoichiometric equation for the oxalate decomposition in vacuum can be written as:



The values of the total pressure calculated using Eq. (10) are presented in the last column of Table 2. There is remarkable agreement with the corresponding total observed pressure values P (using an acetone slurry trap) which justifies the proposed mechanism.

Solid-state reactions occur preferentially in a zone of reactant–product interface that advances through the unreacted solid. The rate of reaction depends not only on the geometric development of the interface but also on the chemistry of interface processes leading to thermal dissociation. With gaseous reaction products an additional factor in terms of ease of escape of the product also contributes to the overall rate, which in turn depends on the rigidity of the reaction domain. When the domain size is small, as in the present case with finely grained anhydrous STO, the inter-domain space provides an easy route of escape for gaseous products. As a result, the products escape as soon as they are formed resulting in a rapid initial rate of reaction. The Zhuravlev equation [10] is based on a model of instantaneous nucleation with three-dimensional growth, where the interface geometry is proportional to amount of unreacted solid. This is in conformity with the absence of an induction period and the

lack of influence of pre-crushing and irradiation on the reaction rate. Once the bulk of gaseous products is released, the grain boundaries suffer major realignment and the matrix is densified. The subsequent prolonged step is attributed to slow diffusion of gaseous products through the gradually densifying matrix.

Acknowledgements

The authors express gratitude to Dr. A.K. Galwey for academic help and advice. We also thank the staff of the Electron Microscopy Unit of Queen's University, Belfast, for obtaining the electron micrographs. One of the authors (S.D.B.) is thankful to the Association of Commonwealth Universities for a fellowship, which made the work possible.

References

- [1] P.K. Gallagher, F. Shrey, *J. Am. Ceram. Soc.* 46 (1963) 567.
- [2] P.K. Gallagher, J. Thomson Jr., *J. Am. Ceram. Soc.* 48 (1965) 644.
- [3] G. Pfaff, F. Schmidt, W. Ludwig, A. Feltz, *J. Therm. Anal.* 33 (1988) 771.
- [4] F.S. Gallaso, *Structure Properties and Preparation of Perovskite Type Compounds*, Pergamon Press, Oxford, 1969.
- [5] E.C. Subba Rao, in: C.N.R. Rao (Ed.), *Solid State Chemistry*, Marcel Dekker, New York, 1974.
- [6] T.T. Fang, H.B. Lin, J.B. Hwang, *J. Am. Ceram. Soc.* 73 (1990) 3363.
- [7] S. Rimlinger, L. Eyraud, P. Eyraud, J.C. Droguet, A. Beauger, *Bull. Soc. Chim. Fr.* 3 (1988) 432.
- [8] I.N. Belyaev, Yu.N. Orlyanskii, *Russ. J. Inorg. Chim.* 17 (1992) 589.
- [9] S.D. Bhattamisra, S. Otta, *J. Therm. Anal.* 41 (1994) 419.
- [10] W.S. Claubach, E.M. Swiggerd, R. Gilchrist, *J. Res. Natl. Bur. Std.* 56 (1956) 289.
- [11] S.D. Bhattamisra, G.M. Laverty, N.A. Baranov, V.B. Okhotnikov, A.K. Galwey, *Phil. Trans. R. Soc. Lond.* 341 (1992) 479.
- [12] M.E. Brown, D. Dollimore, A.K. Galwey, *Comprehensive Chemical Kinetics*, vol. 22, Elsevier, Amsterdam, 1980, p. 70.
- [13] V.V. Boldyrev, I.S. Nev'yantser, Yu.I. Mikhailov, F.F. Khairtdinov, *Kinet. Katal.* 2 (1970) 367.
- [14] G.V. Jere, C.C. Patel, *Ind. J. Chem.* 2 (1964) 383.
- [15] K. Nagase, K. Sato, N. Tanaka, *Bull. Chem. Soc. Jpn.* 48 (1975) 439.
- [16] K. Ceils, I. Van Driessche, R. Mouton, G. Vanhoyland, S. Hoste, *Meas. Sci. Rev.* 1 (2001) 177.
- [17] J. Rak, P. Skurski, M. Gutowski, J. Blazejowski, *J. Therm. Anal.* 43 (1995) 239.
- [18] K. Nagase, *Bull. Chem. Soc. Jpn.* 46 (1973) 144.